RAPID COMMUNICATIONS

PHYSICAL REVIEW B VOLUME 42, NUMBER 4 1 AUGUST 1990

Theoretical electron-positron zone-reduced momentum density for $YBa_2Cu_3O_7$: Fermi surface and wave-function effects

David Singh and W. E. Pickett
Naval Research Laboratory, Washington, D.C. 20375-5000

E. C. von Stetten and Stephan Berko
Department of Physics, Brandeis University, Waltham, Massachusetts 02254
(Received 20 March 1990)

Using the linearized augmented-plane-wave (LAPW) -calculated electron and positron charge densities for $YBa_2Cu_3O_7$, the Brillouin-zone-reduced electron-positron momentum density is computed and the zone-reduced two-dimensional angular correlation of annihilation radiation (2D ACAR) spectrum is produced. The calculations show that the relative weights of the Fermi-surface discontinuities are substantially altered due to the positron preferentially sampling the Cu-O chain region. In addition, the reduced 2D ACAR spectrum contains large **k**-dependent wave-function effects. The theoretical zone-reduced 2D ACAR spectrum is compared to the several existing experimental spectra. It is concluded that, at present, positron-annihilation experiments do not provide consistent and clear evidence for the existence and shapes of Fermi surfaces in $YBa_2Cu_3O_7$.

One of the most critical questions regarding the ground-state electronic structure of the high-T_c superconductors is whether they possess a conventional Fermi surface (FS) in reasonable accord with band-structure calculations.[1,2] Recent photoemission experiments[3] appear to observe a well defined FS in some of these materials. Another method able to resolve the FS of metals not amenable to standard FS studies due to their short electronic mean free paths is the two-dimensional angular correlation of electron-positron annihilation radiation (2D ACAR) technique.[4] Several 2D ACAR experiments have been performed[5,6] on $YBa_2Cu_3O_{7-x}$ samples; some report clear FS signatures,[7,8] while more recent results[9-11] raise questions about the FS interpretation of the 2D ACAR data. It is therefore most important to obtain detailed band theoretical 2D ACAR spectra for comparison with the experimental results regarding the observability of the FS of $YBa_2Cu_3O_7$, should it exist. In this paper we report *ab initio* calculations of the zone-reduced electron-positron (e^--e^+) momentum density $\tilde{\rho}^{2\gamma}(\mathbf{k})$, using the previously calculated[12,13] e^+ charge density in $YBa_2Cu_3O_7$, and discuss the relative importance of the FS versus the wave-function effects on $\tilde{\rho}^{2\gamma}(\mathbf{k})$.

The 2D ACAR technique[4] measures the projection $N_{\hat{\mathbf{n}}}$ of the e^--e^+ momentum density $\rho^{2\gamma}(\mathbf{p})$, $N_{\hat{\mathbf{n}}}(p_x,p_y) = \int dp_z \rho^{2\gamma}(\mathbf{p})$; the projection direction $\hat{\mathbf{n}}$ represents a chosen crystallographic direction. In the independent-particle model (IPM), at zero temperature,

$$\rho^{2\gamma}(\mathbf{p}) = \text{const} \times \sum_{j,\mathbf{k}} n_j(\mathbf{k}) \left| \int d\mathbf{r}\, \psi_+(\mathbf{r}) \psi_{j,k}(\mathbf{r}) e^{i\mathbf{p}\cdot\mathbf{r}} \right|^2 = \text{const} \times \sum_{j,\mathbf{k}} n_j(\mathbf{k}) \sum_{\mathbf{G}} |A_j(\mathbf{k},\mathbf{G})|^2 \delta(\mathbf{p}-\mathbf{k}-\mathbf{G}), \tag{1}$$

where the A_j's are the Fourier coefficients of the thermalized $e^+(\mathbf{k}^+=\mathbf{0})$ and e^- ($\mathbf{k}$,j band index) Bloch-wave product $\psi_+\psi_{j,\mathbf{k}}$, the **G**'s are reciprocal-lattice vectors, and $n_j(\mathbf{k})$ is the electron occupation number of the jth band, reflecting the position of the FS, if any. Thus the FS signatures can be observed as discontinuities in $\rho^{2\gamma}(\mathbf{p})$ —after a reconstruction of the full 3D $\rho^{2\gamma}(\mathbf{p})$ from the projections $N_{\hat{\mathbf{n}}}$—or as discontinuities appearing directly in $N_{\hat{\mathbf{n}}}(p_x,p_y)$. These FS discontinuities, however, are intermixed with potentially large anisotropies in $\rho^{2\gamma}(\mathbf{p})$, due to wave-function modulations. It is therefore usual to perform a "Lock-Crisp-West (LCW) zone folding"[4,14] of the various extended-zone components of $\rho^{2\gamma}(\mathbf{p})$ into the first Brillouin zone, thus forming the zone-reduced momentum density $\tilde{\rho}^{2\gamma}(\mathbf{k}) = \sum_{\mathbf{G}} \rho^{2\gamma}(\mathbf{k}-\mathbf{G})$, to obtain

$$\tilde{\rho}^{2\gamma}(\mathbf{k}) = \text{const} \times \sum_j n_j(\mathbf{k}) \sum_{\mathbf{G}} |A_j(\mathbf{k},\mathbf{G})|^2. \tag{2}$$

In the approximation that the effect of the wave functions on $\tilde{\rho}^{2\gamma}(\mathbf{k})$ via the Fourier coefficients $A_j(\mathbf{k},\mathbf{G})$ varies only slowly with $\mathbf{k}$, $\tilde{\rho}^{2\gamma}(\mathbf{k})$ reflects mainly the FS through the $n_j(\mathbf{k})$'s—the so-called LCW theorem.[14] It was noted[15] that the sum over **G** in Eq. (2) can be reduced to its real-space representation, obtaining

$$\tilde{\rho}^{2\gamma}(\mathbf{k}) = \text{const} \times \sum_j n_j(\mathbf{k}) \int |\psi_+(\mathbf{r})|^2 |\psi_{j,\mathbf{k}}(\mathbf{r})|^2 d\mathbf{r}, \tag{3}$$

i.e., $\tilde{\rho}^{2\gamma}(\mathbf{k})$ is proportional to the IPM annihilation rate of the thermalized positron with the $\psi_{j,\mathbf{k}}$ electrons. The modulation of $\tilde{\rho}^{2\gamma}(\mathbf{k})$ due to wave-function effects in various metals has been studied in several papers.[16]

Since experimental 2D ACAR studies of the FS involve usually the zone-reduced momentum density, we can use Eq. (3) to compute $\tilde{\rho}^{2\gamma}(\mathbf{k})$, leading to a significant computational simplification, since it involves the e^- and e^+ real-space charge densities directly. We thus avoid the computation of the matrix elements $A_j(\mathbf{k},\mathbf{G})$ over the large number of **G**'s needed to insure proper convergence as required by the momentum space expression of $\tilde{\rho}^{2\gamma}(\mathbf{k})$ in Eq. (2). A drawback of this method, however, is the

inability to compare theory directly with the extended-zone 2D ACAR data.

For the calculations reported here, both the electron and positron densities were obtained using the general-potential linearized augmented-plane-wave (LAPW) method.[2] The electron density as a function of $\mathbf{k}$ was calculated for each valence band in the self-consistent potential of Ref. 2, using the convergence parameters reported therein. The e^+ potential was calculated by inverting the Coulomb potential and adding a local approximation to the e^--e^+ correlation potential.[13] Calculations were performed for each valence band on a uniform grid of 121 $\mathbf{k}$ points in the irreducible quarter of the Brillouin zone (BZ) in the $k_z=0$ and $k_z=\frac{1}{2}$ planes. By interpolating between the calculated points for each of the 36 valence bands, additional values were obtained, resulting in a grid of 31×31 points in each plane and 51 points along each of the edges of the quarter BZ's and also along the Γ-S and Z-R directions. Further *ab initio* calculations were carried out at selected points along these lines and in the 31×31 grid in order to check the validity of the interpolation technique. For the contribution of the core and semicore states to the sum in Eq. (3), the electron density was taken to be independent of $\mathbf{k}$, so that only a single calculation was required for these states. We note that the results for the two computed planes were quite similar, due to the low dispersion along the c axis. Similar calculations without the e^--e^+ correlation potential produced only minor differences.[13]

We show our results in Figs. 1 and 2. In Fig. 1(a) (top) the electronic occupation number $\sum_j n_j(\mathbf{k})$ is plotted along several directions in the $k_z=0$ plane of the BZ, exhibiting a unit step at each crossing of a FS. We indicate with double lines the steps at "planelike" Fermi surfaces, while the single-line steps correspond to "chainlike" Fermi surfaces.[1,2] Figure 1(b) shows the corresponding variation of the reduced momentum density $\tilde{\rho}^{2\gamma}(\mathbf{k})$. The difference of $\tilde{\rho}^{2\gamma}(\mathbf{k})$ between the Γ and S points was normalized to that of Fig. 1(a). We note that $\tilde{\rho}^{2\gamma}(\mathbf{k})$ retains sharp steps at the various FS crossings; the amplitudes of the "planelike" steps, however, are substantially reduced compared to the chainlike steps. This effect was expected, since it was shown theoretically[5,12] that the positron samples preferentially the chain region in $YBa_2Cu_3O_7$. In addition to these FS signatures we find a substantial variation in $\tilde{\rho}^{2\gamma}(\mathbf{k})$ as a function of $\mathbf{k}$ between the FS steps, most notably along the Γ (Z)-S (R) directions. This variation is due to the wave-function effects of Eq. (3).

In order to compare our computations with experiments, we have artificially averaged the "a" and "b" directions, obtaining $\tilde{\rho}^{2\gamma}(\mathbf{k})$ for a "twinned" crystal—Fig. 1(c) indicates the result in the $k_z=0$ plane. We then convolute $\tilde{\rho}^{2\gamma}(\mathbf{k})$ with a 2D ACAR Gaussian resolution of full width at half maximum equal to $0.5mc\times10^{-3}$ (the Γ-to-X distance is $3.17mc\times10^{-3}$, $\hbar\equiv1$), obtaining the smooth curve of Fig. 1(d) for $k_z=0$. The existing 2D ACAR spectra[5,7-11] for $YBa_2Cu_3O_{7-x}$ samples were obtained with resolutions of 0.4-$0.8\,mc\times10^{-3}$. In the experiments in which $\rho^{2\gamma}(\mathbf{p})$ is not reconstructed, the projection $\tilde{N}_{\hat{\mathbf{n}}}$ of the reduced momentum density is obtained by direct folding of the projections $N_{\hat{\mathbf{n}}}$, i.e., $\tilde{N}_{\hat{\mathbf{n}}}(k_z,k_y)$ $=\sum_{G_x,G_y}N_{\hat{\mathbf{n}}}(k_x-G_x,\,k_y-G_y)$, where G_x,G_y are the reciprocal lattice vectors of the projected BZ. We obtain $\tilde{\rho}^{2\gamma}(\mathbf{k})$ for the $\mathbf{k}$ points between the two calculated planes by linear interpolation (in view of the small dispersion along c), in order to produce $\tilde{N}_c(k_x,k_y)$ for comparison with experiments in which the projection direction $\hat{\mathbf{n}}$ is chosen along the c axis.[7,9-11] Figure 1(e) shows the resulting $\tilde{N}_c$ after convolution with the same resolution as in Fig. 1(d); the similarity between Fig. 1(d) and Fig. 1(e) indicates again the small c-axis dispersion. For Fig. 1(e), the labels are only indicating the perpendicular BZ projections onto the $k_z=0$ plane.

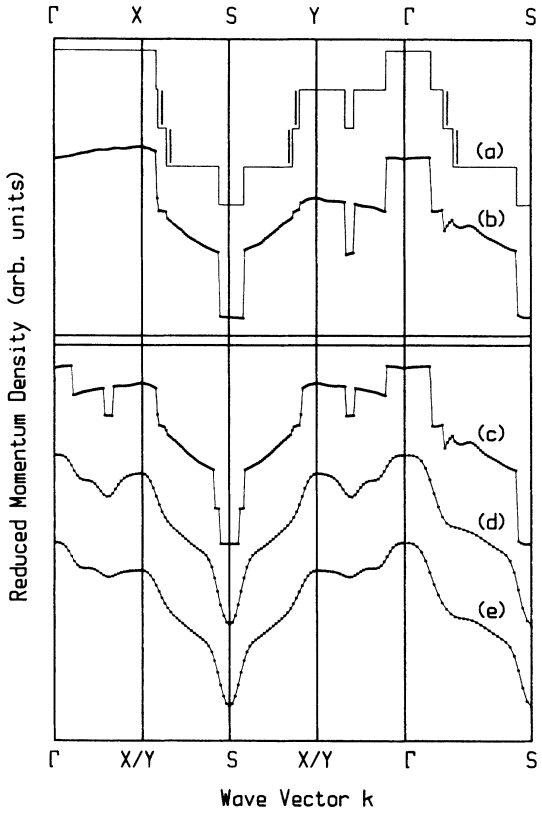

FIG. 1. (a) Theoretical electron occupation number in the $k_z=0$ plane. (b)-(d) The zone-reduced electron-positron momentum density $\tilde{\rho}^{2\gamma}(\mathbf{k})$ as discussed in text: (b) in the $k_z=0$ plane; (c) after averaging the "a" and "b" directions (twinning); (d) same as (c) after convolution with resolution (see text). (e) Projected zone-reduced electron-positron momentum density $\tilde{N}_c(k_x,k_y)$ after convolution with resolution.

In Fig. 2 we show the full two-dimensional shape of the resolution convoluted $\tilde{N}_c(k_x,k_y)$ in perspective (top) and contour line (bottom) plots. We see from Figs. 1(e) and 2 that the $0.5mc\times10^{-3}$ resolution is already sufficient to observe the dominant FS features, i.e., the hole pocket around the S (R) point and the one-dimensional "chain-band"[2] ridge forming a cross centered at the Γ (Z) point due to the averaging of the "a" and "b" directions to simulate twinning. We find, however, that with this resolution the planelike Fermi surfaces are not observable[17] due to their small amplitudes; a resolution of

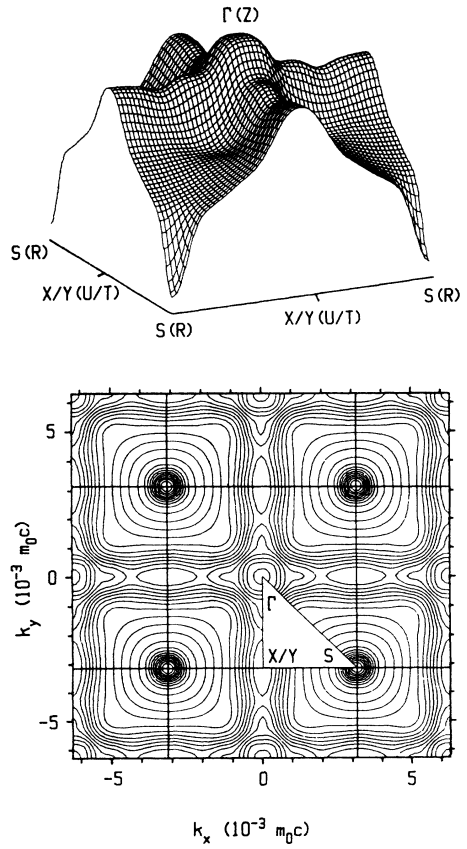

FIG. 2. The projected zone-reduced electron-positron momentum density $\tilde{N}_c(k_x,k_y)$ after convolution with resolution (see text): perspective (top) and contour line plot (bottom). The Brillouin-zone labels as discussed in text.

$\sim 0.2mc\times 10^{-3}$ would begin to reveal these small steps. The significant variation in $\tilde{N}_c$ between the FS "steps" due to the wave-function effects is clearly seen, producing the downward sloping surface from $\Gamma(Z)$ to $S(R)$. We were unable to assign this **k**-dependent wave-function effect to a unique band and conclude that many of the hybridized valence bands contribute to this effect. After including the **k** independent contribution of the core and semicore states, we obtain a variation in $\tilde{N}_c$ from Γ (Z) to S (R) of $\sim$9% of the height at Γ (Z). This predicted magnitude is 2–3 times larger than the variation observed in the experimental $\tilde{N}_c$ spectra. There is general agreement among the various experimental groups regarding the rough behavior of $\tilde{N}_c$, i.e., a tentlike distribution peaked around Γ (Z), decreasing towards the S (R) points. Questions remain, however, about the details of the $\tilde{N}_c$ shapes observed, and thus about the observation of Fermi surfaces. We have also computed the a (b) axis reduced projection $\tilde{N}_{a\,(b)}$ and find a smooth tentlike structure peaked at the center; this distribution is, however, narrower than the published experimental $\tilde{N}_{a\,(b)}$.[5]

In order to study further the observability of the FS "discontinuities" predicted here, we have simulated the effect of counting statistics, i.e., Poisson noise, on the theoretical $\tilde{N}_c$ spectrum.[18] We find that when the data is symmetrized and smoothed, low statistics noise has the effect of introducing shapes into $\tilde{N}_c$ that can overwhelm the FS "images" predicted in Figs. 1 and 2. Our simulations indicate that the experimental 2D ACAR spectra should contain well over 10^7 total counts before the predicted FS signatures can be unambiguously distinguished from noise-produced features. Thus the structures discussed and attributed to FS signatures in Ref. 7 might be at least partially due to noise effects, given the low total counts (4×10^6). The experiments of Ref. 8 involve the reconstruction of the full three-dimensional $\rho^{2\gamma}(\mathbf{p})$, and then the production of the zone-reduced $\tilde{\rho}^{2\gamma}(\mathbf{k})$. Fermi-surface signatures are described, but they differ in shape from each other as well as from those of Ref. 7; except for hole pockets around the S–R line, the details do not follow our theoretical predictions (Fig. 1). Because of the complexity of the different reconstruction algorithms used,[8] and the lack of detailed information regarding total counts, we have not analyzed the effects of noise propagation for such reconstructions. Clearly, more experimental data will be required to reconcile the differences between these experiments;[8] since crystal symmetry is imposed on the data for reconstruction, a careful noise-propagation analysis will also be of importance. Recently published higher statistics [$(50–200)\times 10^6$ total counts] $\tilde{N}_c$ spectra[9,10] seem to indicate essentially no FS "discontinuities." It is to be noted, however, that the absence of clear FS signatures in positron data could be the result of e^+ trapping[5,6] or e^+ localization due to chain disorder[12] in the various samples used by the different groups. Substantial chain disorder may also wash out the FS's of the chainlike bands.[2] Trapping and/or localization could also be responsible for the smaller experimentally observed Γ (Z) to S (R) variation compared to theoretical predictions.

In summary, we conclude that the band theoretical zone-reduced electron-positron momentum density in $YBa_2Cu_3O_7$ is dominated by chainlike FS discontinuities and wave-function modulations throughout the zone. An improvement of at least a factor of 2–3 in experimental resolution would be required to observe the amplitude-reduced planelike FS signatures. In addition, high statistics data is essential in order to reduce effects produced by symmetrization and smoothing of noisy data. At present, the results of the various positron annihilation experiments are unfortunately too contradictory to provide sufficiently clear evidence for the existence and detailed shapes of Fermi surfaces in $YBa_2Cu_3O_7$. The lack of observation of FS discontinuities in the available high statistics data cannot rule out the existence of Fermi surfaces because of possible e^+ trapping in the $YBa_2Cu_3O_7$ crystals used. Even if future high-resolution and low-noise data would unambiguously show the chainlike FS structures in the reduced momentum density spectra, it is clear that high-T_c materials that possess no Cu-O chains would be better candidates to elucidate the existence and shapes of the FS's due to the Cu-O planes that play an essential role in high-T_c superconductivity. Among such materials $Tl_2Ba_2CaCu_2O_8$ seems the most promising,[13] should high-quality single crystals become available.

The work at the Naval Research Laboratory is supported in part by the U.S. Office of Naval Research, and at Brandeis University by National Science Foundation Grant No. DMR-88-14185. Computations were carried out under the auspices of the National Science Foundation at the Cornell National Supercomputer Facility. One of us (D.S.) would like to acknowledge support from the National Research Council.

[1]J. Yu, S. Massidda, A. J. Freeman, and D. D. Koelling, Phys. Lett. A **122**, 203 (1987).

[2]H. Krakauer, W. E. Pickett, and R. E. Cohen, J. Supercond. **1**, 111 (1988).

[3]A. J. Arko *et al.*, Phys. Rev. B **40**, 2268 (1989); C. G. Olson *et al.*, Science **245**, 731 (1989); J. C. Campuzano *et al.*, Phys. Rev. Lett. **64**, 2308 (1990).

[4]See reviews in *Positron Solid State Physics,* edited by W. Brandt and A. Dupasquier (North-Holland, New York, 1983); S. Berko, in *Momentum Distributions,* edited by R. N. Silver and P. E. Sokol (Plenum, New York, 1989), p. 273.

[5]See, for example, the reviews by A. A. Manuel, J. Phys. Condens. Matter **1**, SA107 (1989); M. Peter, L. Hoffmann, and A. A. Manuel, in *Positron Annihilation,* edited by L. Dorikens-van Praet, M. Dorikens, and D. Segers (World Scientific, NJ, 1989), p. 197.

[6]S. Berko, in *High T_c Superconductors: Magnetic Interactions*, edited by L. H. Bennett, Y. Flom, and G. C. Vezzoli (World Scientific, NJ, 1989).

[7]L. C. Smedskjaer, J. Z. Liu, R. Benedek, D. G. Legnini, D. J. Lam, M. D. Stahulak, H. Claus, and A. Bansil, Physica **C156**, 269 (1988).

[8]M. Peter, L. Hoffmann, and A. A. Manuel, Physica **C153-155**, 1724 (1988); S. Tanigawa, in *Positron Annihilation,* Ref. 5, p. 119; and (unpublished).

[9]M. Peter and A. A. Manuel, Phys. Scr. **T29**, 106 (1989).

[10]H. Haghighi, J. H. Kaiser, S. Rayner, R. N. West, M. J. Fluss, R. H. Howell, P. E. A. Turchi, A. L. Wachs, Y. C. Jean, and Z. Z. Wang, J. Phys. Condens. Matter **2**, 1911 (1990).

[11]AT&T Bell Laboratories, Brandeis University, Brookhaven National Laboratory 2D ACAR Collaboration, P. Sferlazzo *et al.* (unpublished).

[12]E. C. von Stetten, S. Berko, X. S. Li, R. R. Lee, J. Brynestad, D. Singh, H. Krakauer, W. E. Pickett, and R. E. Cohen, Phys. Rev. Lett. **60**, 2198 (1988).

[13]D. Singh, W. E. Pickett, R. E. Cohen, H. Krakauer, and S. Berko, Phys. Rev. B **39**, 9667 (1989).

[14]D. G. Lock, V. H. C. Crisp, and R. N. West, J. Phys. F **3**, 561 (1973).

[15]N. Shiotani, Solid State Phys. (Tokyo) **19**, 526 (1984); Z. Szotek and W. M. Temmerman (private communication).

[16]See for example, L. P. L. M. Rąbou and P. E. Mijnarends, Solid State Commun. **52**, 933 (1984); J. H. Kaiser, R. N. West, and N. Shiotani, J. Phys. F **16**, 1307 (1986).

[17]We note two other band calculations of $\tilde{\rho}^{2\gamma}$ along selected lines in the BZ [A. Bansil, P. E. Mijnarends, and L. C. Smedskjaer, Bull. Am. Phys. Soc. **35**, 427 (1990); S. Massidda *et al.* (unpublished)] that are in rough agreement with the results reported here in the two full planes. There are some differences, however, in the amplitudes and positions of the "plane" vs "chain-like" FS's among these calculations. A previous linear muffin-tin orbitals calculation (Ref. 9) of $\tilde{N}_c$ disagrees with the overall experimental trends.

[18]Details of the noise simulation results will be published in a more extended paper.